

Transparent (Ni,Au)/ZnO:Al-Based Ohmic Contacts to p-Type GaN as an Insight into the Role of Ni and Au in Standard p-Type GaN Contacts

Aleksandra Wójcicka, Zsolt Fogarassy, Tatyana Kravchuk, Cecile Saguy, Eliana Kamińska, Piotr Perlin, Szymon Grzanka, and Michał Adam Borysiewicz*



Cite This: <https://doi.org/10.1021/acsami.4c12850>

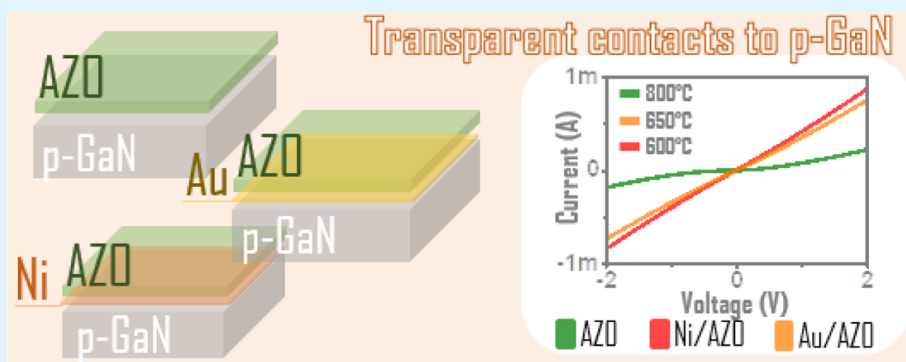


Read Online

ACCESS |

Metrics & More

Article Recommendations



ABSTRACT: In this work, Ni/ZnO:Al and Au/ZnO:Al structures are proposed as efficient ohmic contacts to p-GaN. Through a careful selection of deposition parameters and annealing environment, we not only achieve the formation of high-quality ohmic contacts but also gain insights into the interfacial reactions, enhancing the understanding of conventional Ni/Au contact formation on p-GaN. In particular, the notion that the presence of NiO at the interface is enough for an ohmic contact to form is challenged by showing that in fact it has to be NiO formed at the interface from metallic Ni and additional oxygen. An Au-based ohmic contact is also presented, and its formation mechanism is explained, contrary to popular knowledge that Au does not form an ohmic contact with p-GaN. The obtained contacts are low resistivity, with contact resistances of $4.77 \times 10^{-3} \Omega \cdot \text{cm}^2$ and $3.34 \times 10^{-3} \Omega \cdot \text{cm}^2$ for Au-based and Ni-based ones, respectively. What is also important is that we show these oxide-based contacts with metallic interlayers give lower series resistances in simplified diode structures than a standard Ni/Au-based contact, making them promising for optoelectronic devices.

KEYWORDS: gallium nitride, transparent conductive oxide, AZO, ohmic contact, GaN, sputtering, subcontact layers, interface engineering

INTRODUCTION

Although GaN-based optoelectronics and electronics are already well established commercially and have been studied for several decades, there are still issues regarding some individual technology steps, which could be optimized, as evidenced by a large publication output in the field. In particular, the challenge of fabricating high quality ohmic contacts is still not completely overcome.^{1–5} All bipolar GaN-based devices, whether lateral or vertical, must have good ohmic contacts with Ga-face p-GaN for efficient operation. Generally, ohmic contacts to p-GaN require high work function metals such as Pt, Pd, Au, or Ni, in the form of layered structures, e.g., Ni/Au,⁶ Pt/Au,⁷ Cr/Au,⁸ Pt/Ni/Au,⁹ etc. The standard metallization stack for such applications is the Ni/Au bilayer, annealed to form the contact in a nitrogen–oxygen mixture at around 500 °C. Such contacts, although

exhibiting low resistivities in the range $10^{-4} \div 4 \times 10^{-6} \Omega \cdot \text{cm}$,^{6,10} limit the performance of optoelectronic devices such as light-emitting diodes (LEDs) or laser diodes (LDs) as the metallic character of the contact stack introduces light scattering and absorption issues. To counter these effects, transparent conductive oxides (TCOs) have begun to be explored with the most common TCO, SnO:In (ITO) showing promising results as p-type contact in GaN-based

Received: July 31, 2024

Revised: October 22, 2024

Accepted: October 22, 2024

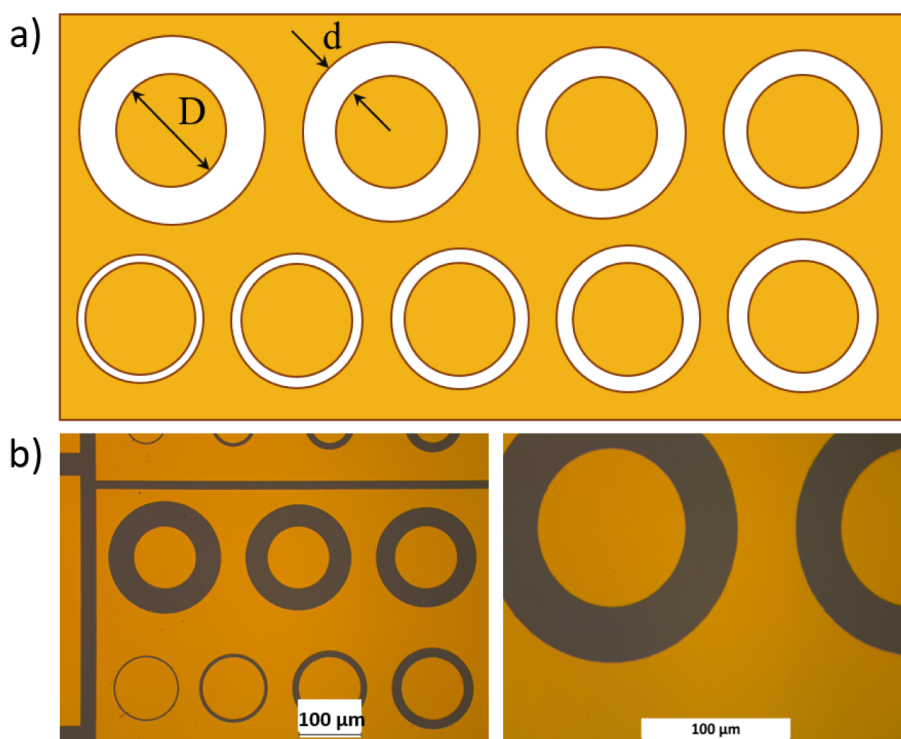


Figure 1. CTLM patterns (a) used to calculate specific contact resistance, D is the diameter of the inner circle and is $100\ \mu\text{m}$, d widths vary and are, respectively, 40, 35, 30, 25, 20, 15, 10, 5, and $2\ \mu\text{m}$. Optical microscope photograph (b) at 20 \times and 50 \times magnification.

LDs.^{11–13} ITO is a well-known TCO, which is widely applied as a transparent electrode in the display industry owing to its low resistivity of around $10^{-4}\ \Omega\cdot\text{cm}$ and high transparency with more than 90% in the blue and visible wavelength region. However, the disadvantages of ITO, such as high refractive index, scarcity, and high costs of indium, have resulted in a strong effort to replace it in all applications. The best candidate for this task is ZnO:Al (AZO) which is earth-abundant and can reach resistances low enough for most applications. Importantly for GaN-based devices, the physical properties of ZnO are significantly better matched to GaN than those of ITO. Both GaN and ZnO have a hexagonal crystal structure, with similar a lattice parameters of 3.189 and 3.25 Å,¹⁴ respectively, as opposed to the cubic ITO with a lattice parameter of 10.12 Å.¹⁵ The thermal expansion coefficients are also similar for ZnO: $4.31 \times 10^{-6}\ \text{K}^{-1}$ and GaN: $3.43 \times 10^{-6}\ \text{K}^{-1}$,¹⁴ as opposed to the one for ITO: $10.2 \times 10^{-6}\ \text{K}^{-1}$.¹⁵ Such a mismatch can cause both static and thermal strain, leading to faster degradation of GaN/ITO devices than when GaN/AZO is used. However, to date, there are only a couple of works on AZO application in ohmic contacts to p-GaN. Chen et al.¹⁶ showed a contact with AZO directly deposited by e-beam deposition at 350 °C on p-GaN structures on a sapphire substrate. Although the Mg acceptor concentration in the p-type film as well as the hole concentrations measured by the Hall effect are relevant to appropriately judge the quality of the contacts, they are not stated in this work. The authors achieve a high contact resistivity of $2.19 \times 10^{-2}\ \Omega\cdot\text{cm}^2$ after formation in a nitrogen ambient at 500 °C for 1 min. Han et al.¹⁷ deposited an Ag/AZO bilayer onto Mg-doped p-GaN structures on sapphire. The hole concentration in the films was around $1 \times 10^{17}\ \text{cm}^{-3}$. The 2 nm Ag and 200 nm AZO layers were deposited by using e-beam deposition at room temperature. The contacts were formed at 600 °C in air, and

the specific resistivity reached was equal to $9.76 \times 10^{-4}\ \Omega\cdot\text{cm}^2$. It is worth highlighting that in both reports the I – V traces were not ideally ohmic around 0 V bias. This feat was achieved by Su et al.¹⁸ who employed a new technique for AZO deposition—a two-step approach with a spin-coated interface: the AZO film was deposited first, followed by atomic layer deposition of a thicker AZO. The first film aimed at lowering the current flow barrier at the interface, while the second aimed at lowering the series resistance of the contact. The method required temperature formation stages at different steps reaching 600 °C in air for 2 h. The final contact was formed at 600 °C after annealing in nitrogen for 1 min. The substrate was an unspecified p-GaN template with a hole concentration of $1.2 \times 10^{17}\ \text{cm}^{-3}$. The final contact resistivity was again quite high at $1.47 \times 10^{-2}\ \Omega\cdot\text{cm}^2$. Some of the lowest contact resistivities were reported by Lin et al.¹⁹ while using MOCVD to deposit AZO on top of p-GaN doped with Mg to an unknown level, topped off with a Si-doped n+ InGaIn layer with $3 \times 10^{20}\ \text{cm}^{-3}$. The deposition temperature was 400 °C, and the achieved resistivities were equal to $2.72 \times 10^{-4}\ \Omega\cdot\text{cm}^2$. While this value is very low, the deposition technique is quite complex. Finally, a very recent report by Slimani Tlemcani et al.²⁰ claims that by applying a 5-nm thick Ni interlayer under AZO it is possible to obtain very low resistivity contacts to p-GaN, reaching $1.85 \times 10^{-4}\ \Omega\cdot\text{cm}^2$, after formation annealing at 500 °C in air for 5 min. A p-GaN/GaN/sapphire structure was used with Hall-determined hole concentrations equal to $4 \times 10^{17}\ \text{cm}^{-3}$. Ni was deposited by e-beam evaporation, and the AZO film was deposited by radio frequency (RF) sputtering in pure argon. The authors explain the contact formation through the creation of a p-NiO film, which should lead to the barrier lowering to p-GaN. While this can be a valid explanation for some cases, it has to be noted that in their report the presented I – V traces are not perfectly linear, and thus the presented

discussion on the formation of a truly ohmic contact is lacking. Generally, the role of NiO in the contacts to p-GaN has been discussed for years and still has not been determined definitively, with different reports showing contradicting behavior.

In this report, we employ the AZO/interlayer/p-GaN structure as a microlaboratory to investigate the interfacial reactions under precisely selected contact formation conditions. Using advanced characterization techniques, we aim to understand the processes occurring at the interface and elucidate why the mere presence of NiO is insufficient to form an ohmic contact. By forming the contact in a nitrogen atmosphere rather than in oxygen, the source of oxygen in the interfacial reaction is confined exclusively to the AZO. Additionally, we apply varying base pressure as a minute source of oxygen for the Ni as well as deposit directly a p-NiO film to discuss the difference between the simple presence of NiO as-deposited and the on-interface formation of NiO. To detach from the chemical properties of the Ni, we discuss a contact with a similar interlayer made of Au—a metal with an almost identical work function as Ni—and show, based on the ion diffusion considerations, how the form factors influence the contact behavior. Taking all into account, we add to the deconvolution of the role of Ni in the widely used contact formation to p-GaN and at the same time present a new AZO/Au/p-GaN contact scheme and show that both AZO/Ni/p-GaN and AZO/Au/p-GaN have better performance in device structures than the standard Ni/Au-based contact.

■ EXPERIMENTAL DETAILS

To prepare ohmic contacts, p-GaN substrates were grown by metal-organic vapor phase epitaxy (MOVPE) on sapphire. The GaN structure consisted of 2 μm -thick unintentionally doped GaN (UID-GaN), 550-nm thick Mg-doped GaN with a dopant concentration of $1 \times 10^{19} \text{ cm}^{-3}$, and 10-nm thick heavily Mg-doped with a dopant concentration of $2 \times 10^{20} \text{ cm}^{-3}$. After activation annealing of the GaN structures, Hall measurement data showed a hole concentration of $3.8 \times 10^{17} \text{ cm}^{-3}$. The fabrication of contacts started with the cleaning of the p-GaN substrate in organic solvents, i.e., boiling trichloroethylene, acetone, and isopropanol, to remove any contamination that could potentially interfere with subsequent processes. Since the AZO developed by us has been shown to have record low resistivity when deposited at room temperature using magnetron sputtering,²¹ the patterning of the contact structures could be done by lift-off photolithography. Circular transmission line method (cTLM) patterns (see Figure 1a) were therefore prepared in the photoresist on the cleaned GaN structures. Prior to introduction in the vacuum chamber, each sample was bathed in a 1:2 HCl:H₂O solution for 3 min at room temperature, followed by a 3 min deionized water rinse to remove the native oxide. We prepared several sets of samples starting with 100 nm AZO deposited directly onto p-GaN.

The AZO source was a ceramic target with the standard composition of 98 wt % ZnO and 2 wt % Al₂O₃ (Plasmaterials, Inc., USA), which was sputtered in pure argon under 200 W DC power and 0.5 Pa at room temperature, as described in ref. 21. Next, samples with a 2.5 nm Ni interlayer between the AZO and p-GaN were prepared in the same way, with Ni and AZO deposited consecutively without breaking the vacuum. The source of Ni was a metallic target. To study the influence of oxygen presence during film growth on NiO formation and contact formation, we prepared a second sample with the same structure, but this time deposited at a slightly worse base vacuum—yielding two samples, one deposited at 10^{-5} Pa and the other at 10^{-4} Pa. Furthermore, we decided to fabricate a sample with a p-NiO interlayer deposited completely in oxygen to see if the direct deposition of NiO, argued to be the decisive factor in contact formation, would, in fact, create an as-

deposited ohmic contact. The NiO was deposited using a NiO target in the RF mode, under the conditions yielding p-type material, i.e., 0.5×10^{-2} Pa total pressure, sputtering gas: pure oxygen, current 200 mA. Prior to the contact fabrication, NiO films with a 150 nm thickness were deposited on quartz to confirm p-type conductivity—the hole concentration was $1.5 \times 10^{19} \text{ cm}^{-3}$, and the mobility was $5 \text{ cm}^2 \text{ V}^{-1} \text{ s}^{-1}$. As will be seen in the results discussion, there are effects that might be related to the nanostructural form factor of the interfacial material, which is why we fabricated another sample with no Ni whatsoever, but with a slightly thicker Au film (4 nm). Au is a noble metal with a similar work function as nickel, 5.15 eV for Au and 5.1 eV for Ni. This means that Au should not take part in any reaction at the interface, but its electronic properties can have an impact. We treat the gold therefore as a probe of a metal similar to Ni in terms of electronic properties, but without its reactivity to oxygen in particular to try and deconvolute the physical properties, of the metal at the interface from the chemical ones. To facilitate electrical measurements, 30-nm thick Au metallizations were deposited as a top contact by a Leica ACE 600 sputter coater. Finally, a reference 100 nm Au/20 nm Ni/p-GaN sample was prepared without any AZO, since it is a standard p-type contact. After lift-off, all of the contacts underwent forming annealing. All AZO-containing contacts were formed in pure nitrogen flow for 90 s at temperatures starting from 200 °C and reaching formation temperature, which was different, depending on each sample. We did not go over 800 °C, since these temperatures may lead to the degradation of the LD or LED quantum well sequence in GaN devices for which the transparent contacts were designed. If ohmic character was seen for lower temperatures, we did not increase the annealing temperature further for the same reason. The furnace used was a Mattson SHS 100 rapid thermal processing furnace. We intentionally chose not to form the AZO-containing contacts in air nor to deposit the AZO in an oxygen containing atmosphere, to see if the oxygen from the AZO film itself would be enough to convert any of the Ni to NiO. The reference Ni/Au contact was formed in the typical conditions at 500 °C, in an 80% nitrogen:20% oxygen atmosphere for 5 min.

The structural analysis of the samples was performed by X-ray diffraction with a Cu cathode in the Bragg–Brentano configuration on a PANalytical Empyrean system. *I*–*V* measurements were conducted using a Keithley 2400 source-meter, and the cTLM analysis was done using an approach published elsewhere.²² The (scanning) transmission electron microscopy ((S)TEM) examinations were carried out in an aberration-corrected THEMIS microscope at 200 keV. For the energy-dispersive X-ray spectroscopy (EDS) mapping, a Super-X detector was used. The cross-sectional TEM specimens were prepared by a focused ion beam (FIB) technique. Since the FIB uses Ga ions for specimen thinning, small amounts (1–2%) of this Ga could remain in the sample across its thickness, which is why the Ga outdiffusion was not analyzed using EDS mapping but secondary ion mass spectroscopy. Depth profiles at the interface were measured by time-of-flight secondary ion mass spectroscopy (TOF-SIMS) in a TOF-SIMS 5 (of IONTOF GmbH) system. Both negative and positive ion depth profiles were recorded. The sputtering was done for the negative analysis using 2 kV Cs⁺ ions and for the positive analysis using 2 kV O₂⁺ ions, while in both cases, the analysis beam was formed of 25 kV Bi⁺ ions.

■ RESULTS AND DISCUSSION

The *I*–*V* characteristics of the reference Au/Ni/p-GaN contact after deposition and after formation are shown in Figure 2a. The trend is fully linear, and the specific contact resistivity extracted from cTLM is $4.3 \times 10^{-4} \Omega \cdot \text{cm}^2$. This value, even if different from some literature reports, is low and will be the benchmark for this experiment as the arguably best Ni-based contact resistivity that could be achieved for p-GaN. We will treat it as a measure of how good the contact can be with the p-GaN structure we use. In Figure 2b, the *I*–*V* characteristics of the AZO/p-GaN contact are shown for different formation

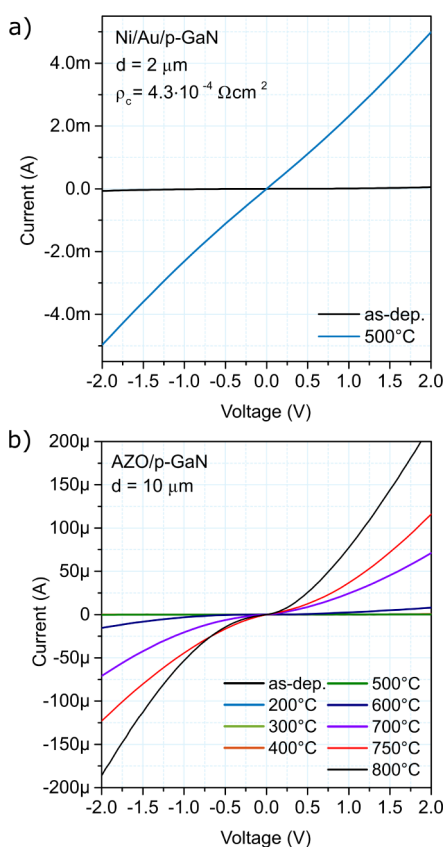


Figure 2. I – V characteristic of (a) the reference contact to p-GaN annealed at 500 °C and (b) AZO contact to p-GaN after heat treatment at temperatures from 200 to 800 °C.

temperatures. The characteristics are symmetric against the 0 V bias point, linear at high bias, and nonlinear for lower bias. A narrowing of the nonlinearity range can be seen with increasing formation temperature, reaching around ± 1 V after formation at 800 °C. The nonlinearity shows there is a potential barrier at the interface, which needs to be overcome by electrical polarization. The lowering of the bias range indicates some sort of reaction at the interface, which leads to a lowering of the barrier. The currents increase with increasing annealing temperature, indicating a lowering of the contact resistance itself as well as of the electrode series resistance. The latter is typical for AZO, which upon annealing tends to increase in conductivity. Since the contact was not fully linear, no value of contact resistance could be determined, but for comparison, one can note that the currents at ± 2 V bias are around 0.2 mA.

Based on TOF-SIMS depth profiles presented in Figure 3d,e, we can say that after deposition there seems to be no mixing between AZO and GaN with sharp interfaces between the ZnO^- and GaN^- profiles. After annealing at 800 °C, the main difference that can be seen is a significant Ga outdiffusion to the AZO as visible when comparing the Ga^+ and GaN^- profiles in the AZO layer for both cases; the intensity of the former increases by almost 2 orders of magnitude, while the intensity of the latter remains unchanged. In the negative mode, the CN^- peaks correspond to nitrogen and are present at all interfaces. After annealing, the first sharp peaks lower their intensity and become wider at all interfaces. We cannot therefore clearly say that this would be nitrogen outdiffusion. In the case of AZO, it is also unlikely, since the oxide does not have such an affinity for nitrogen as the commonly used

metals. Additional details on the interface reactions are uncovered from (S)TEM data. A very nice epitaxial ZnO layer is observed in the as deposited sample, Figure 3a. The planes of ZnO (0002) are parallel to the surface, while in most areas of the sample, the planes of ZnO (11–20) lie parallel to the planes of GaN (110). Almost one single crystal of ZnO was deposited. The lattice distances of GaN (11–20) and ZnO (11–20) are 0.157 and 0.163 nm, respectively. Due to the good fit, one orientation became dominant in the majority of the layer, but ZnO particles with different orientations were also observed. In the sample after formation annealing at 800 °C, perfect epitaxy could be seen, based on which the formation of a single crystal ZnO layer is presumed. The orientation relationship between the ZnO layer and the GaN substrate is the same as that in the as-deposited sample. In contrast, to the as-deposited sample, EDS studies did not show a homogeneous Al distribution (Figure 3b,c). Areas of 10–20 nm can be detected in the layer, where the concentration of Al is slightly higher than its surrounding area. A higher concentration of Al layer (one or two atoms thick) was also detected on the surface of GaN. Based on the TOF-SIMS, (S)TEM, and EDS data, it looks like two effects are observed in the contact—Ga outdiffusion creating V_{Ga} in GaN and the formation of an Al monolayer at the interface. V_{Ga} is a deep acceptor in GaN,²³ and Al is a shallow donor in ZnO, meaning that the formation annealing leads to the creation of a $\text{GaN}(p+)$ /AZO($n++$) tunnel junction contact.

Addition of Ni at the interface enables ohmic contact formation and improves the I – V characteristics after annealing at 600 °C. Compared to AZO/p-GaN contacts, the AZO/Ni/p-GaN contacts are fully linear in all the range with 4 times higher currents—around 0.8 mA at ± 2 V (see Figure 4a), and the specific contact resistivity can be determined at $3.34 \times 10^{-3} \Omega \cdot \text{cm}^2$. The temperature of formation is also much lower than that for pure AZO and is much more acceptable for LD/LED technology. In the XRD patterns measured for increasing formation temperatures, we can see that apart from the GaN (0002) substrate peak superimposed with the AZO (0002) peak due to their epitaxial relationship and the Au (111) peak from the top gold layer, a peak around 44° begins to appear at 500 °C and grows stronger with increasing temperature as shown in Figure 4b. It can be related to either Ni (111) or NiO (200). (S)TEM imaging was used to obtain further information on the interface in this case. In the as-deposited sample, a 3-nm thick Ni layer is observed on the surface of the GaN substrate, followed by a columnar crystallized ZnO layer. An oxidized Zn–Ni layer with a few atomic layers' thickness is observed between the GaN and Ni layers (see Figure 4c). After annealing, NiO islands are formed with a 9–13 nm thickness. Between the islands, Zn (O,N) is present at the interface in an amorphous form. Above that interfacial layer, the columnar ZnO remains (Figure 4d). Looking closely at the EDS maps, one can see that in the NiO, the oxygen signal has a lower level than in the AZO film. It might therefore be true that it is more of a Ni-rich NiO, or strongly O-deficient NiO than pure p-type NiO. It is generally accepted that Ni-vacancies are acceptors in NiO that are responsible for the p-type conductivity of the material. In this case, we could have much more oxygen vacancies, which are known as hole killers in NiO.²⁴ TOF-SIMS depth profiles (see Figure 5) add more information to the already complex picture. Interestingly, no increase in the Ga level in AZO can be seen, indicating that the outdiffusion of Ga from GaN is not taking place in this case. On the other

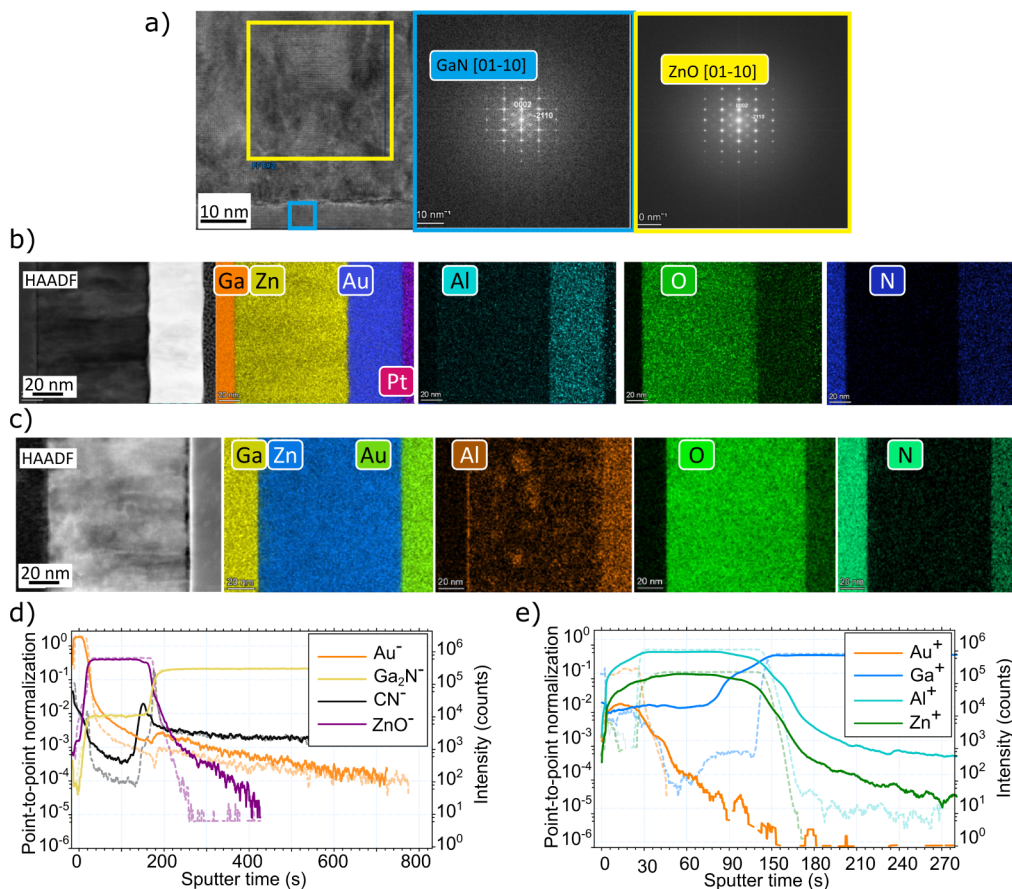


Figure 3. (a) HR-TEM images of the AZO/p-GaN interface with FFT images from color-coded areas. Epitaxy of AZO and GaN can be seen. (b) High-angle annular dark field image (HAADF) and EDS elemental maps of the as-deposited AZO/GaN contact. (c) HAADF and EDS images of the AZO/p-GaN contact after formation at 800 °C. Positive ion (d) and negative ion (e) TOF-SIMS depth profiles of AZO/p-GaN contacts after deposition (dashed lines) and after contact formation at 800 °C (solid lines).

hand, the Ni⁺ peak does diffuse significantly, both into GaN as well as out through AZO and into the Au cap after annealing. Looking at the negative depth profiles, both Ni⁻ and NiO⁻ can be seen, albeit slightly shifted, with Ni⁻ directly at the interface and in the substrate and NiO⁻ from the side of the AZO layer. The peaks also cover parts of one another, which leads to the conclusion that the contact is a complex structure of AZO/NiO/Ni_{1-x}O_{1-x}/Ni/p-GaN with holes in the Ni-containing trilayer. We were not able, however, using the available techniques and due to the changing Ni/NiO peak ratios in space, to identify directly the atomic ratios of Ni to O. To see if a slight increase in the oxygen content during deposition would influence the contact behavior, we opted to prepare the same structure under conditions with poorer base vacuum in the deposition chamber. A poorer vacuum means more residual gases such as air, water vapor, and hydrocarbons impinging on the substrate before and during growth. In the standard base vacuum used in our experiments, 10⁻⁵ Pa, a surface will be covered by a monolayer of contaminant roughly in 25 s. Lowering the vacuum by an order of magnitude will yield the same coverage in only 2.5 s. The 2.5-nm thick Ni film has roughly 7 atomic layers with a 0.352 nm lattice spacing. The deposition of the Ni took around 5 s. Therefore, with a 10⁻⁵ Pa base pressure, the Ni/contaminant ratio in the film would be around 2.8%, whereas under 10⁻⁴ Pa, it would be around 28%, showing much more pronounced oxidation. The AZO was deposited with a rate of 2.9 nm·s⁻¹, and we found no influence

of background pressure on its resistivity—an AZO film deposited on a quartz substrate had a resistivity of around $2 \times 10^{-3} \Omega\cdot\text{cm}^2$ with the variation within $\pm 10\%$. The contact deposited at a poorer base vacuum was formed under the same conditions and also yielded a fully ohmic I - V characteristic, but this time the specific contact resistivity was much lower, at $6.16 \times 10^{-4} \Omega\cdot\text{cm}^2$, comparable to the resistivity of our fully metallic Ni/Au reference contact. It would therefore seem that more oxidation would be better for the contact, as more Ni is converted to NiO. Additionally, the previous work on AZO/Ni/p-GaN contact²⁰ claims that it is the presence of NiO which changes the band alignment of the whole contact stack in a way enabling the ohmic character of the junction. With that in mind, we tested an AZO/p-NiO/p-GaN contact with NiO deposited from a NiO target under 100% oxygen gas. Interestingly, while the NiO was present, the contact performance was almost nonexistent with strongly nonlinear, asymmetric I - V characteristics and maximum currents around 100 nA. This shows that it is not enough to just have NiO at the interface and that the band alignment hypothesis is false. Our results show that it is in fact a mixture of metallic and oxidized nickel that yields ohmic contact formation through an interfacial reaction and in situ oxidation.

Finally, to include other potential nanoscale mechanisms in the contact stack, the AZO/Au/p-GaN stack was studied. Au is a Schottky barrier to GaN with a typical barrier height around 0.55–0.6 eV.²⁵ This is true in the case of regular thickness

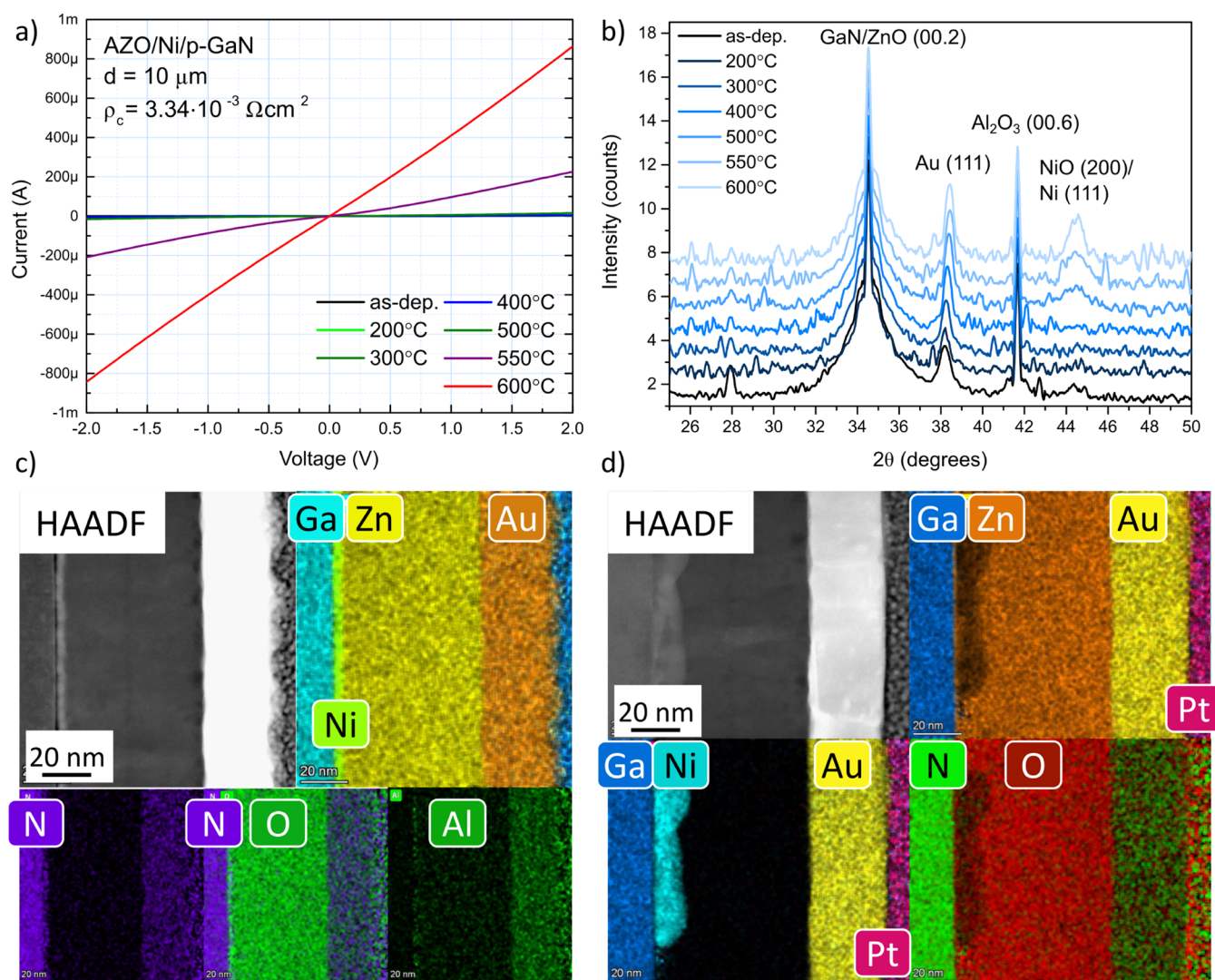


Figure 4. I – V characteristics (a) and XRD patterns (b) of the AZO/Ni/p-GaN sample as a function of the heat treatment temperature. HAADF and EDS elemental maps of the AZO/Ni/p-GaN contact after deposition (c) and after ohmic contact formation at 600 °C (d).

electrodes of tens of nanometers in breadth. The phenomena observed at the nanoscale with our 4 nm-thick Au film are noteworthy. Without any Ni presence whatsoever, the AZO/Au/p-GaN contact yielded ohmic character after annealing at 650 °C (see Figure 6a) and a specific contact resistivity of $4.77 \times 10^{-3} \Omega \cdot \text{cm}^2$, only slightly higher than our high vacuum AZO/Ni/p-GaN contact. The onset of increased currents starts at 500 °C, when in the XRD patterns a peak at 37° starts to appear (see Figure 6b). It can be identified as Au (111), the strongest of the Au XRD peaks. Its non-Lorentzian shape is indicative of the nanocrystalline character of the film. (S)TEM data showed that the initially uniform Au film is broken up into patches of tens of nanometers in width, with ZnO penetrating the spaces between the patches (see Figure 6c,d). Again, as in the case of the AZO/Ni/p-GaN, we have these direct AZO/p-GaN contact areas; however, the current performance of the whole structure evidences much lower current flow resistances than in the pure AZO/p-GaN structure and at lower temperatures. However, similar Ga^+ outdiffusion can be seen as that for AZO/p-GaN, which was absent from the Ni-containing contact. This creates again a V_O -rich subcontact region in p-GaN. On the other hand, the Au profile in TOF-SIMS shown in Figure 6e only broadens indicative of the

recrystallization seen in (S)TEM. This creates a case where a metallic phase is present in intimate connection to a p++ region in the GaN, leading to a tunneling ohmic contact. This situation is different from that of pure AZO/p-GaN in the fact that here, the tunneling takes place directly to the high work function metal through a thin potential barrier in the valence band. In AZO/p-GaN, the tunneling occurs between p++ and n++ regions of semiconductors; hence, it has to be assisted by tunneling to local in-gap states, the efficiency of which is lower yielding higher resistance and nonohmicity.²⁶

As a final test of the contact performance, we processed test laser structures with AZO/Ni/p-GaN, AZO/Au/p-GaN, the reference Pt/Au/Ni/p-GaN top contacts, and standard Au/Ni/Al/Ti/n-GaN bottom contacts. The current–voltage characteristics are shown in Figure 7a. It can be seen that the general shape and threshold currents are similar for all of the samples. The currents are higher for samples with AZO-based contacts. The series resistances of the contacts extracted from the characteristics show that all contacts have resistances of a similar order with the Ni/AZO ones having the lowest values improving on the reference metallic contact (see Figure 7b). Bearing in mind the transparency of the AZO, this proves

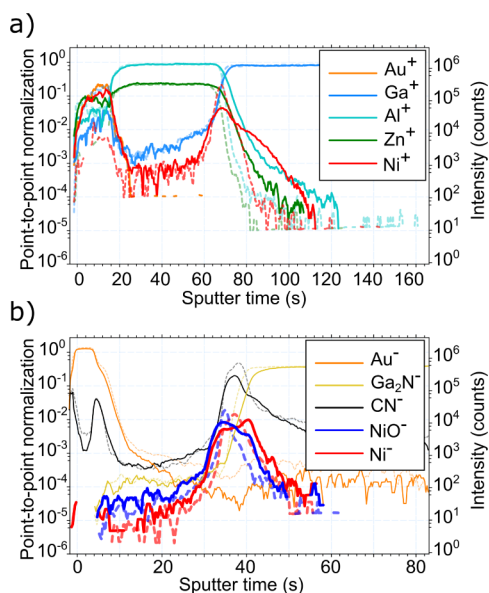


Figure 5. TOF-SIMS depth profiles for the AZO/Ni/p-GaN sample taken with positive ions (a) and negative ions (b).

the viability of this approach to contact formation and their applicability in optoelectronic devices.

CONCLUSIONS

We demonstrate a system of a new type of ohmic contacts to p-GaN for LED/LD applications with sustainability in mind. The AZO-based electrodes with Ni and Au interlayers form ohmic contacts to p-GaN after nitrogen flow annealing at low temperatures of 600 and 650 °C, respectively. The obtained contact resistances are promising at $3.34 \times 10^{-3} \Omega\text{-cm}^2$ for an AZO/Ni/p-GaN stack and $4.77 \times 10^{-3} \Omega\text{-cm}^2$ for an AZO/Au/p-GaN stack. What is also important is that we treat this system as a vehicle to understand the role of Ni in the formation of conventional Ni/Au ohmic contacts to p-GaN. By having only AZO and background process pressure as the oxygen source in the experiment, we were able to perform controlled oxidation of the interfacial nanolayers and check its influence on the contact performance. We found that Ni is partially oxidized after contact formation, however with the Ni signal separate from NiO still visible in the TOF-SIMS profiles close to the GaN surface. Depositing the same AZO/Ni/p-GaN contact in a poorer base vacuum leading to substantial residual gas contamination and oxidation of the Ni, actually lowered the contact resistance to $6.16 \times 10^{-4} \Omega\text{-cm}^2$, comparable to the resistance of our Au/Ni/p-GaN reference contact. We excluded the necessity for full Ni oxidation by depositing a highly p-type NiO film instead of a Ni interlayer. Such an AZO/NiO/p-GaN stack had almost no transverse conductivity, showing that the Ni should be somewhat oxidized but not fully. Finally, studies of the AZO/Au/p-

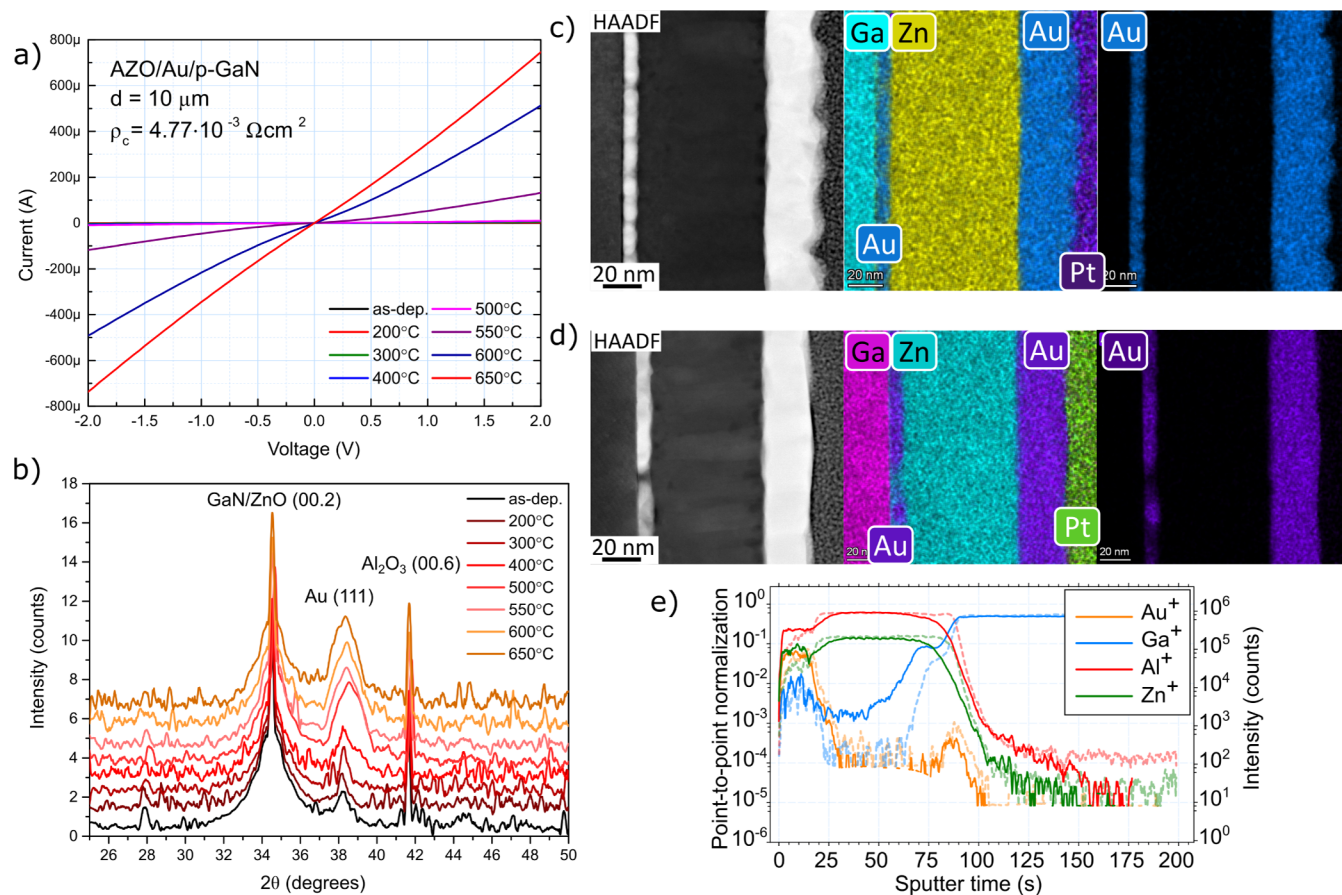


Figure 6. *I*–*V* characteristics (a) and XRD patterns (b) of the AZO/Au/p-GaN sample as a function of the heat treatment temperature. HAADF and EDS elemental maps of the AZO/Au/p-GaN contact after deposition (c) and after ohmic contact formation at 650 °C (d). (e) TOF-SIMS depth profiles for the AZO/Ni/p-GaN sample, measured for positive ions.

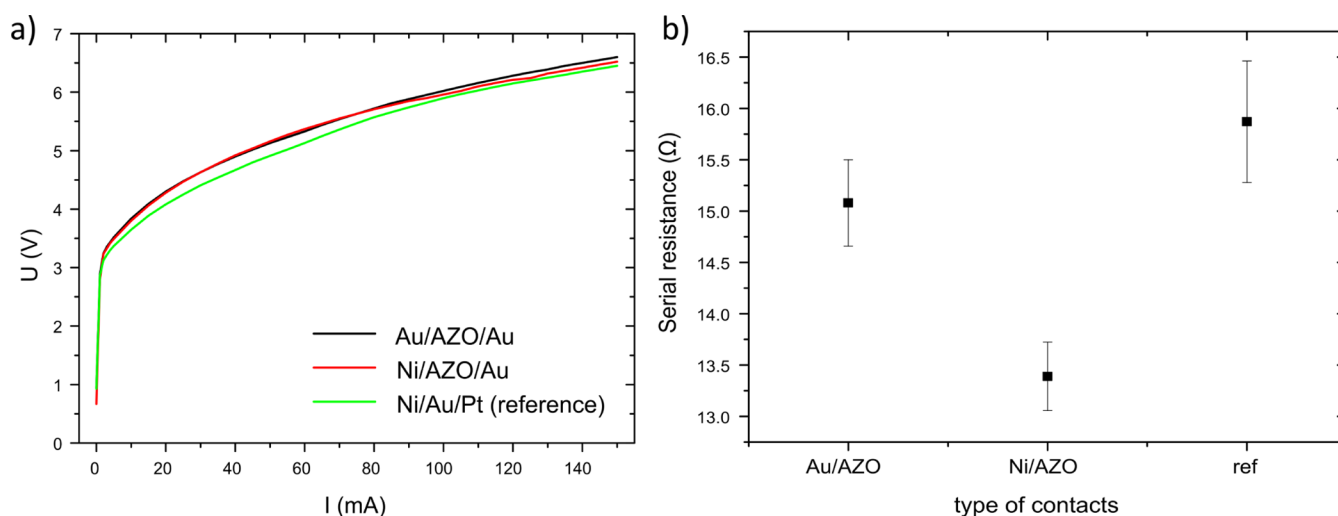


Figure 7. I – V characteristics of simplified laser diodes (a) and the series resistance values extracted from them (b) for devices with AZO/Ni/p-GaN, AZO/Au/p-GaN, the reference Pt/Au/Ni/p-GaN top contacts and standard Au/Ni/Al/Ti/n-GaN bottom contacts.

Table 1. TCO-Based Ohmic Contacts to p-GaN for GaN-Based Light Emitting Devices

Contact	Annealing conditions	Contact resist. ($\Omega \cdot \text{cm}^2$)	Ref.
60 nm ITO	$\text{N}_2/600 \text{ }^\circ\text{C}/1'$	3×10^{-2}	27
60 nm ITO	$\text{N}_2/600 \text{ }^\circ\text{C}/1'$	1.6×10^{-2}	28
AZO	$\text{N}_2/500 \text{ }^\circ\text{C}/1'$	2.19×10^{-2}	16
AZO bilayer	air/600 $^\circ\text{C}/2 \text{ h}$	1.47×10^{-2}	18
2 nm Ag/200 nm AZO	air/600 $^\circ\text{C}/1'$	9.76×10^{-4}	17
2.5 nm Ni/100 nm AZO	$\text{N}_2/600 \text{ }^\circ\text{C}/30 \text{ s}$	3.34×10^{-3}	this work
4 nm Au/100 nm AZO	$\text{N}_2/650 \text{ }^\circ\text{C}/30 \text{ s}$	4.77×10^{-3}	this work

GaN stack, where Au has almost the same work function as Ni, but none of its oxygen-reactivity suggested that outdiffusion of Ga from the subcontact region can be an important aspect in the creation of contact; however, this mechanism was not present for the Ni-based contact, where the Ga outdiffusion was not seen in TOF-SIMS profiles. To summarize, we believe we have shown that the picture of ohmic contact formation through NiO formation at the interface is not sufficient, as nonoxidized Ni has some additional role to play. Additionally, the creation of V_{Ga} should not be regarded as happening in all cases, nor necessary for ohmic contact formation. Finally, we show a valid way to make ohmic contacts to light-emitting devices based on GaN, with properties on par with other TCO-based solutions; see Table 1.

AUTHOR INFORMATION

Corresponding Author

Michał Adam Borysiewicz – Łukasiewicz Research Network, Institute of Microelectronics and Photonics, Warsaw 02-668, Poland; orcid.org/0000-0002-7661-2412; Email: michal.borysiewicz@imif.lukasiewicz.gov.pl

Authors

Aleksandra Wójcicka – Łukasiewicz Research Network, Institute of Microelectronics and Photonics, Warsaw 02-668, Poland; orcid.org/0000-0003-0846-8890

Zsolt Fogarassy – Institute for Technical Physics and Materials Science, Centre for Energy Research, Budapest 1121, Hungary

Tatyana Kravchuk – Technion - Israel Institute of Technology, Haifa 3200003, Israel

Cecile Saguy – Technion - Israel Institute of Technology, Haifa 3200003, Israel

Eliana Kamińska – Institute of High Pressure Physics, Polish Academy of Sciences, Warsaw 01-142, Poland

Piotr Perlin – Institute of High Pressure Physics, Polish Academy of Sciences, Warsaw 01-142, Poland

Szymon Grzanka – TOP-GAN, Warsaw 01-142, Poland

Complete contact information is available at:

<https://pubs.acs.org/10.1021/acsami.4c12850>

Author Contributions

A.W. contributed to writing—review and editing, writing—original draft, investigation, formal analysis, and data curation. Z.F., T.K., C.S., E.K., P.P., and S.G. contributed to writing—review and editing, investigation, formal analysis, and data curation. M.A.B. contributed to writing—review and editing, writing—original draft, validation, supervision, resources, project administration, methodology, investigation, funding acquisition, formal analysis, data curation, and conceptualization.

Notes

The authors declare no competing financial interest.

ACKNOWLEDGMENTS

This work was supported by the National Centre for Research and Development, Poland, project ‘OxyGaN’ M-ERA.NET/2019/6/2020, by the Hungarian NRDI Fund, grant number 2019 2.1.7 ERA NET 2020 00002, and by the Israel Ministry of Science, Technology and Space in the frames of the M-era.net Programme. The Hungarian authors thank the support of VEKOP-2.3.3-15-2016-00002 of the European Structural

and Investment Funds. This paper was also supported by the János Bolyai Research Scholarship of the Hungarian Academy of Sciences. The authors wish to thank Dr Andrzej Taube for help with the current–voltage characterization and determination of the reference contacts.

REFERENCES

- (1) Zhang, M.; Ikeda, M.; Huang, S.; Liu, J.; Zhu, J.; Zhang, S.; Yang, H. Ni/Pd-based ohmic contacts to p-GaN through p-InGaN/p⁺-GaN contacting layers. *J. Semicond.* **2022**, *43*, 092803.
- (2) Su, H.; Zhang, T.; Xu, S.; Lu, J.; Du, H.; Tao, H.; Zhang, J.; Hao, Y. Mechanism of low Ohmic contact resistance to p-type GaN by suppressed edge dislocations. *Appl. Phys. Lett.* **2022**, *120*, 222101.
- (3) Tang, C. Y.; Lu, H. H.; Qiao, Z. P.; Jiang, Y.; Du, F. Z.; He, J. Q.; Jiang, Y. L.; Wang, Q.; Yu, H. Y. Ohmic Contact with a Contact Resistivity of 12 Ω mm on p-GaN/AlGaIn/GaN. *IEEE Electron Device Lett.* **2022**, *43*, 1412–1415.
- (4) Wang, J.; Lu, S.; Cai, W.; Kumabe, T.; Ando, Y.; Liao, Y.; Honda, Y.; Xie, Y. H.; Amano, H. Ohmic Contact to P-Type GaN Enabled by Post-Growth Diffusion of Magnesium. *IEEE Electron Device Lett.* **2022**, *43*, 150–153.
- (5) Fogarassy, Z.; Wójcicka, A.; Cora, I.; Rácz, A. S.; Grzanka, S.; Dodony, E.; Perlin, P.; Borysiewicz, M. A. Structural and electrical investigation of Al/Ti/TiN/Au based N-face n-GaN contact stack. *Mater. Sci. Semicond. Process* **2024**, *175*, 108250.
- (6) Ho, J. K.; Jong, C. S.; Chiu, C. C.; Huang, C. N.; Chen, C. Y.; Shih, K. K. Low-resistance ohmic contacts to p-type GaN. *Appl. Phys. Lett.* **1999**, *74*, 1275–1277.
- (7) King, D. J.; Zhang, L.; Ramer, J. C.; Hersee, S. D.; Lester, L. F. Temperature behavior of Pt/Au ohmic contacts to p-GaN. *Materials Research Society Symposium - Proceedings. MRS Online Proc. Libr.* **1997**, *468*, 421.
- (8) Trexler, J. T.; Pearton, S. J.; Holloway, P. H.; Mier, M. G.; Evans, K. R.; Karlicek, R. F. Ni/Au, Comparison of Pd/Au, Cr/Au metallizations for ohmic contacts to p-GaN. *Materials Research Society Symposium - Proceedings, MRS Online Proc. Libr.* **1996**; *499*, 1091.
- (9) Jang, J. S.; Chang, I. S.; Kim, H. K.; Seong, T. Y.; Lee, S.; Park, S. J. Low-resistance Pt/Ni/Au ohmic contacts to p-type GaN. *Appl. Phys. Lett.* **1999**, *74*, 70–72.
- (10) Chen, L. C.; Ho, J. K.; Jong, C. S.; Chiu, C. C.; Shih, K. K.; Chen, F. R.; Kai, J. J.; Chang, L. Oxidized Ni/Pt and Ni/Au ohmic contacts to p-type GaN. *Appl. Phys. Lett.* **2000**, *76*, 3703–3705.
- (11) Sung, Y. J.; Kim, M.-S.; Kim, H.; Choi, S.; Kim, Y. H.; Jung, M.-H.; Choi, R.-J.; Moon, Y.-T.; Oh, J.-T.; Jeong, H.-H.; Yeom, G. Y. Light extraction enhancement of AlGaIn-based vertical type deep-ultraviolet light-emitting-diodes by using highly reflective ITO/Al electrode and surface roughening. *Opt. Express* **2019**, *27*, 29930.
- (12) Weisbuch, C.; Speck, J. S.; Nakamura, S.; DenBaars, S. P.; Becerra, D. L.; Zhang, H.; Mehari, S.; Cohen, D. A. *Semipolar III-nitride laser diodes for solid-state lighting*; SPIE, 2019; p 15.
- (13) Mehari, S.; Cohen, D. A.; Becerra, D. L.; Weisbuch, C.; Nakamura, S.; Denbaars, S. P. Optical gain and loss measurements of semipolar III-nitride laser diodes with ITO/thin-p-GaN cladding layers. In *2018 76th Device Research Conference (DRC)*, IEEE: 2018; pp. 1–2.
- (14) Hanada, T. *Basic Properties of ZnO, GaN, and Related Materials*, Springer: 2009; pp. 1–19.
- (15) Choi, S. K.; Lee, J. I. Effect of film density on electrical properties of indium tin oxide films deposited by dc magnetron reactive sputtering. *J. Vac. Sci. Technol., A* **2001**, *19*, 2043–2047.
- (16) Chen, P. H.; Chen, Y. A.; Chang, L. C.; Lai, W. C.; Kuo, C. H. Low operation voltage of GaN-based LEDs with Al-doped ZnO upper contact directly on p-type GaN without insert layer. *Solid-State Electron.* **2015**, *109*, 29–32.
- (17) Han, T.; Wang, T.; Gan, X. W.; Wu, H.; Shi, Y.; Liu, C. Low resistance and transparent Ag/AZO ohmic contact to p-GaN. *J. Korean Phys. Soc.* **2014**, *65*, 62–64.
- (18) Su, X.; Zhang, G.; Wang, X.; Chen, C.; Wu, H.; Liu, C. Two-step deposition of Al-doped ZnO on p-GaN to form ohmic contacts. *Nano Res. Lett.* **2017**, *12*, 469.
- (19) Lin, J.-Y.; Pei, Y.-L.; Zhuo, Y.; Chen, Z.-M.; Hu, R.-Q.; Cai, G.-S.; Wang, G. High-performance InGaIn/GaN MQW LEDs with Al-doped ZnO transparent conductive layers grown by MOCVD using H₂O as an oxidizer. *Chinese Phys. B* **2016**, *25*, 118506.
- (20) Slimani Tlemcani, T.; Mauduit, C.; Bah, M.; Zhang, M.; Charles, M.; Gwoziecki, R.; Yvon, A.; Alquier, D. Development of Low-Resistance Ohmic Contacts with Bilayer NiO/Al-Doped ZnO Thin Films to p-type GaN. *ACS Appl. Mater. Interfaces* **2023**, *15*, 8723–8729.
- (21) Wójcicka, A.; Fogarassy, Z.; Rácz, A.; Kravchuk, T.; Sobczak, G.; Borysiewicz, M. A.; Wang, G. Multifactorial investigations of the deposition process - Material property relationships of ZnO: Al thin films deposited by magnetron sputtering in pulsed DC, DC and RF modes using different targets for low resistance highly transparent films on unheated. *Vacuum* **2022**, *203*, 111299.
- (22) Sadowski, O.; Kamiński, M.; Taube, A.; Tarenko, J.; Guziejewicz, M.; Wzorek, M.; Maleszyk, J.; Jóźwik, I.; Szerling, A.; Prystawko, P.; et al. Low-Resistivity Ti/Al/TiN/Au Ohmic Contacts to Ga- and N-Face n-GaN for Vertical Power Devices. *Phys. Status Solidi (a)* **2024**, *2400076*.
- (23) Neugebauer, J.; Van de Walle, C. G. Gallium vacancies and the yellow luminescence in GaN. *Appl. Phys. Lett.* **1996**, *69*, 503–505.
- (24) Egbo, K. O.; Liu, C. P.; Ekuma, C. E.; Yu, K. M. Vacancy defects induced changes in the electronic and optical properties of NiO studied by spectroscopic ellipsometry and first-principles calculations. *J. Appl. Phys.* **2020**, *128*, 135705.
- (25) Lu, S.; Deki, M.; Kumabe, T.; Wang, J.; Ohnishi, K.; Watanabe, H.; Nitta, S.; Honda, Y.; Amano, H. Lateral p-type GaN Schottky barrier diode with annealed Mg ohmic contact layer demonstrating ideal current-voltage characteristic. *Appl. Phys. Lett.* **2023**, *122*, 142106.
- (26) Okumura, H.; Martin, D.; Malinverni, M.; Grandjean, N. Backward diodes using heavily Mg-doped GaN growth by ammonia molecular-beam epitaxy. *Appl. Phys. Lett.* **2016**, *108*, 072102.
- (27) Kim, T. K.; Yoon, Y. J.; Oh, S. K.; Lee, Y. L.; Cha, Y. J.; Kwak, J. S. Ohmic Contact Mechanism for RF Superimposed DC Sputtered-ITO Transparent p-Electrodes with a Variety of Sn₂O₃ Content for GaN-Based Light-Emitting Diodes. *Appl. Surf. Sci.* **2018**, *432*, 233–240.
- (28) Cha, Y.-J.; Lee, G. J.; Lee, Y. L.; Oh, S. K.; Kwak, J. S. Temperature-Dependent Contact Resistivity of Radio Frequency Superimposed Direct Current Sputtered Indium Tin Oxide Ohmic Contact to p-Type Gallium Nitride. *Thin Solid Films* **2015**, *591*, 182–185.